JMEPEG (2012) 21:105–113
DOI: 10.1007/s11665-010-9820-0

1059-9495/$19.00

# Development and Characterization of Electrocodeposited Nickel-Based Composites Coatings

*L. Kodandarama, M. Krishna, H.N. Narasimha Murthy, and S.C. Sharma*

*(Submitted June 21, 2010; in revised form September 6, 2010)*

**The objective of the article is to study the development and characterization of composite coatings using nickel-tungsten carbide (Ni-WC), nickel-silicon carbide (Ni-SiC), nickel-carbon black (Ni-CB), and nickel-carbon nanotube (Ni-CNT) materials using electrocodeposition technique by varying the composition of reinforcements. The electrochemical parameters such as current density, bath temperature, and pH of the solution were maintained at constant levels for all the coating configurations. The composition of the coating and its proportion were studied using x-ray diffraction and energy dispersive x-ray spectroscopy, respectively. Mechanical properties such as ultimate tensile strength and microhardness were studied. Morphology of the coatings and fracture surfaces were studied using scanning electron microscope. Improvement in mechanical properties of composite coatings was found due to the reduction in crystalline size of the composites coatings. Although loading of carbon nanotube was the least, it also shows good mechanical properties along with Ni-WC composite coatings.**

**Keywords** electrocodeposition, mechanical properties, Ni composite coating

## 1. Introduction

Interest in electrocodeposition of nickel-based composite coatings has increased in recent years due to their unique combination of wear, magnetic, electrical, and corrosion properties (Ref 1). In general, composite coatings reinforced with hard oxide or carbide particles such as $Al_2O_3$, $TiO_2$, $SiO_2$, SiC, and WC or even diamond improves their wear resistance and reduces friction wear (Ref 2-4). Non-metallic inclusion such as WC and SiC in the metal changes its electron structure and crystal lattice that result in changes in the physical and mechanical properties of the electro-deposits (Ref 5, 6). On the other hand, metallic deposits such as carbon black (CB) and carbon nanotubes (CNT) incorporated in the metal through electrocodeposition result in formation of clusters. The electric fields are stronger around the CB/CNT clusters, than in other areas, which may result in increased local deposition rates and higher current densities. Under higher current densities, the differential depositing rates lead to a coarser surface. This may affect the mechanical properties of the composite coatings (Ref 7).

Several researchers have reported on electrodeposition of ceramic (SiC/WC) (Ref 8, 9) and metallic (CB/CNT) (Ref 6-10) reinforcements to improve hardness, wear, and corrosion properties. Only a few research works (Ref 3, 11) focus on mechanical properties of composite coatings, specifically Ni-WC composite coatings. However, comparative studies between electrocodeposited composite coatings using ceramic and metallic reinforcements are not reported in literature. This work studies the effect of the reinforcements such as SiC, WC, CB, and CNT on the morphology and mechanical properties of the electrocodeposited composite coatings.

**L. Kodandarama, M. Krishna,** and **H.N. Narasimha Murthy**, Research and Development, Department of Mechanical Engineering, R V College of Engineering, Bangalore, India; and **S.C. Sharma**, Centre for Advanced Materials, Tumkur University, Tumkur, Karnataka, India. Contact e-mails: krishna_phd@yahoo.co.in and scsrvrd@yahoo. co.in.

## 2. Experimental

Analytical reagents and double-distilled water were used to prepare the plating solution. The reinforcement, bath temperature, bath current, and loading levels were maintained as per the procedure reported by Hachemi et al. (Ref 8). The reinforcements such as WC, SiC, CB, and CNT were added to the bath in different proportions, after the bath attained a uniform temperature of 50 °C.

The reinforcement powder (WC/SiC/CB/CNT) was added to the bath at different concentrations shown in Table 1. The electrolyte and reinforcement blend were sonicated in an ultrasonic bath to ensure sufficient wetting and uniform dispersion of reinforcement particles in the electrolyte. After sonication the suspension was transferred to an electrolyzer and diluted to the required concentration. The pH value was corrected by means of sodium-hydroxide or sulfuric-acid solution as required. The plating solution was agitated during electro-deposition with a magnetic stirrer for an hour. The electromotive force of laminar fluid flow directed the reinforced particles to the cathode surface and prevented them from sedimentating on the bulk of electrode. Before each experiment one surface of the MS plate (dimension as given

**Table 1 Dispersion materials and operation parameters of Ni-based Composite coatings**

| | Dispersion materials | | | |
|---|---|---|---|---|
| | **WC** | **SiC** | **CB** | **CNT** |
| Particle dimension, μm | 1-2 | 5-10 | 0.150-0.225 | 0.09-dia 3-length |
| Chemical (quantity g/L) | | | | |
| $NiSO_4$ $6H_2O$ | 250 | 90 | 260 | 260 |
| $NiCl_2$ $6H_2O$ | 35 | 3 | 35 | 35 |
| $H_3BO_3$ | 40 | 40 | 40 | 40 |
| Particle loading | 2, 4, and 6 | 10, 15, and 20 | 0.5, 1.0, and 1.5 | 0.2, 0.4, and 0.6 |
| Sodium lauryl sulfate | | 2 | 2-6 | 2-6 |
| Thallium sulfate | | 0.5 | | |
| Saccharine | | | 0.5 | 0.5 |

| **Operational parameters** | | | | |
|---|---|---|---|---|
| **Current density** | **Bath temperature** | **pH** | **Stirring speed** | **Plating time** |
| 4 $A/dm^2$ | 50 °C | 4 | 250 rpm | 60 min |

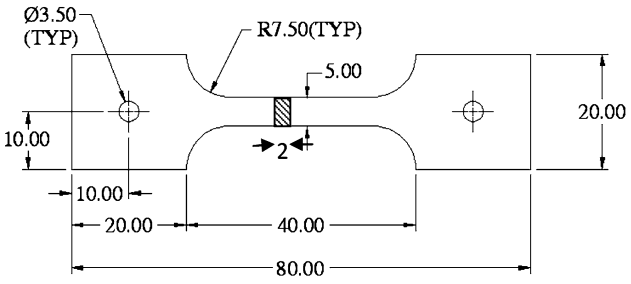


**Fig. 1** Dimension of the tensile samples (all dimension are in mm)

in Fig. 1) was polished to grade 2400 with emery papers, rinsed in distilled water, activated with 5% sulfuric acid at room temperature, and finally ultrasonically degreased with acetone. Electro-deposition was carried out on vertical electrodes with the distance between the cathode and the anode maintained at 90 mm for all experiments. Plating was carried out at specified temperature for 1 h in all cases. The laminar flow condition during electro-deposition was ensured using a magnetic stirrer.

After electrolysis, the deposits on MS plate were ultrasonically cleaned in distilled water for 10 min to remove loosely held reinforcement particles from the surface. The embedded reinforced particles were evaluated using energy dispersive x-ray spectroscopy (EDS) and the quantity of reinforced particles and Ni deposition were determined based on the mean value of at least three measurements for each deposit. The thicknesses of the coatings were measured using an Elektro Physik thickness gauge. Measurements of the Vickers microhardness (HV in $kgf\,mm^{-2}$) of pure nickel and Ni-based composite deposits were performed on the surface using a Reichert microhardness tester and the corresponding final values were determined averaged over 10 measurements. The load for microhardness testing was selected under 1000 g so as to avoid any substrate effect on the microhardness value. Morphological and microstructural characterizations of the deposits were carried out using scanning electron microscopy. The preferred crystalline orientation of the Ni was examined by applying x-ray diffraction (XRD) technique using a JEOL JDX-8030 x-ray diffractometer System.

Tensile tests to examine coating strength were carried out using universal testing machine at constant strain rate of 0.1 mm/min. The dimensions of tensile specimen are shown in Fig. 1.

$$\sigma_c = \frac{F_c - F_m}{t_c \times w_c} \qquad \text{(Eq 1)}$$

Tensile tests were carried out for all nickel and nickel-based composites coatings as given in Eq 1. Here, $\sigma_c$ is the stress of coating layer at particular strain, MPa; $F_c$ and $F_m$ are the loads taken by coated specimen and uncoated specimen, respectively, at particular strain; and $t_c$ and $W_c$ are the coating thickness and coating width, respectively, in mm.

## 3. Results and Discussion

Figure 2(a) to (e) shows the morphology of the deposited specimens with Ni (4 $A/dm^2$, 55 °C), Ni-WC(4 $A/dm^2$, 55 °C, WC-4 g/L), Ni-CB (4 $A/dm^2$, 55 °C, CB-0.5 g/L), Ni-CNT (4 $A/dm^2$, 55 °C, CNT-0.2 g/L), and Ni-SiC (4 $A/dm^2$, 55 °C, SiC-20 g/L) composite coatings. SEM micrographs of the Ni coating shown in Fig. 2(a) exhibit a homogeneous metallic structure of pure Ni with a typical shape of nickel crystallites, which may exceed a size 5 μm.

From Fig. 2(b) it can be observed that the WC particles are homogeneously dispersed in the Ni-WC film. The figure also shows the reduction grain size of Ni crystallites due to the presence of WC reinforcement. This reduction is also discernible in SEM micrographs of composite deposits as compared with those of pure Ni deposits even though some of them have formed agglomerated clusters. Both Ni-CB and Ni-CNT coating surface morphology was very rough as observed in Fig. 2(c) and (d) respectively. The possible reasons for the coarse surface under larger current density are many voids or gaps in the deposits of Ni-CB and Ni-CNT apart from clusters of CNTs/ CB are seen in the deposited Ni layers. Also, notice the uneven distribution of the deposition current density due to

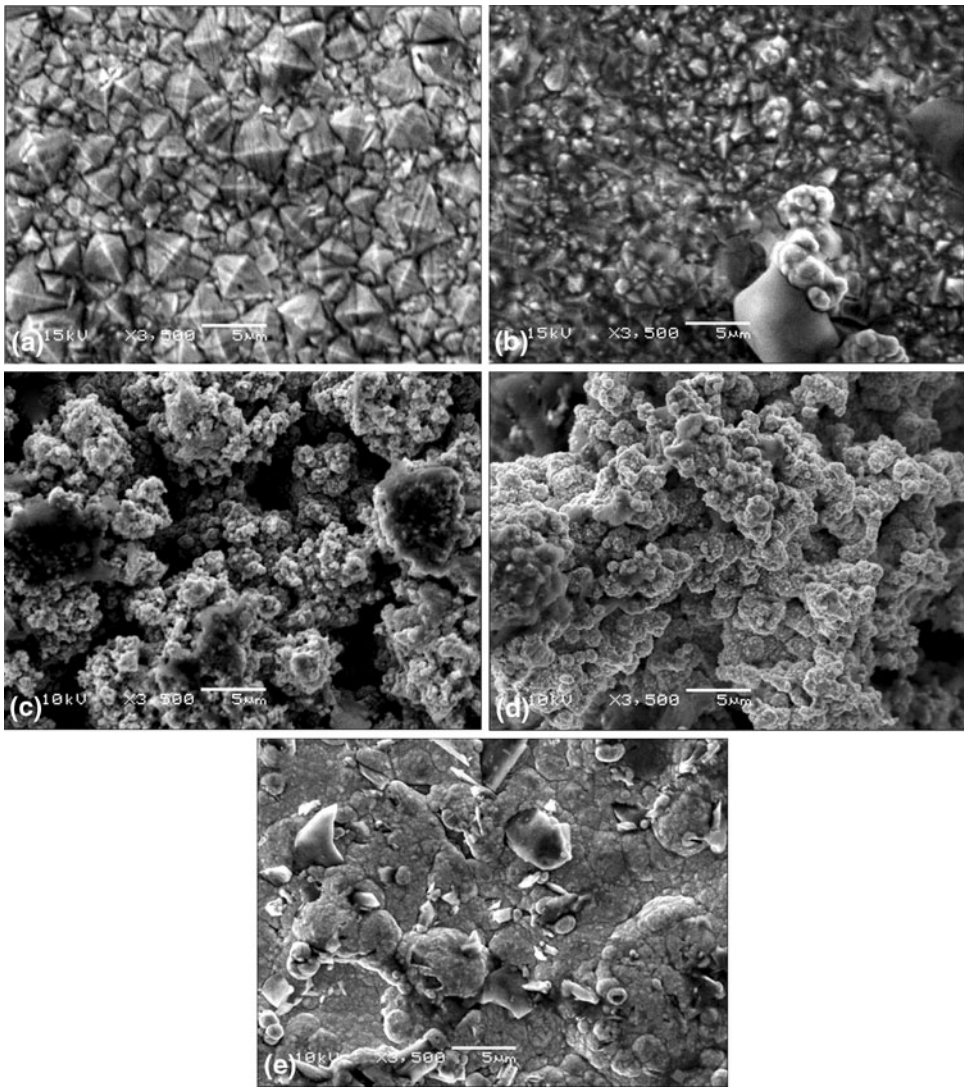


**Fig. 2** Microstructure of Ni-based coatings on MS plate. (a) Ni coating, (b) Ni-WC coating, (c) Ni-CB coating, (d) Ni-CNT coating, and (e) Ni-SiC coating

the existence of CB/CNTs. CB/CNT that are good conductors with a small radius of curvature radius. This fact results in an electric field is stronger around the cluster of CB/CNTs the than in other areas, resulting in increased local deposition current densities during electro-co-deposition and leading to an uneven coating thickness.

Figure 2(e) shows Ni-SiC grains that are smaller than 1 μm with some globular grain-agglomerates visible on the surface.

Table 2 shows the effect of bath loading on the percentage weight (wt.%) of reinforcement in the composite coating by computing from EDS results (as shown in Fig. 3). The wt.% of reinforcement in the coating in CB and CNT are proportional to loading content in the composite plating bath, but WC and SiC reinforcements showed lower wt.% in the coating. Coating with smaller particles (CB and CNT) exhibited higher activity than coating with larger particles (WC and SiC). This may be attributed to the fact that heavy particles are difficult to be carried by the Ni ions due to lower effect of their throwing power (Ref 12). wt.% of reinforcement in the coating increased with increasing bath loading. The other reason for increasing the CNT/CB concentration in the alloy was to check (a) whether conductivity of reinforcement increased the throwing power, (b) the deposition rate improves the properties of the

**Table 2 Approximate wt.% of reinforcement in the Ni coatings computed by EDS**

| | | | |
|---|---|---|---|
| WC loading | | | |
| Loading in g/L | 2 | 4 | 6 |
| wt.% | 0.55 | 2.11 | 3.87 |
| CB loading | | | |
| Loading in g/L | 0.5 | 1 | 1.5 |
| wt.% | 0.35 | 0.95 | 1.214 |
| CNT loading | | | |
| Loading in g/L | 0.2 | 0.4 | 0.6 |
| wt.% | 0.163 | 0.318 | 0.515 |
| SiC loading | | | |
| Loading in g/L | 10 | 15 | 20 |
| wt.% | 2.13 | 3.78 | 4.25 |

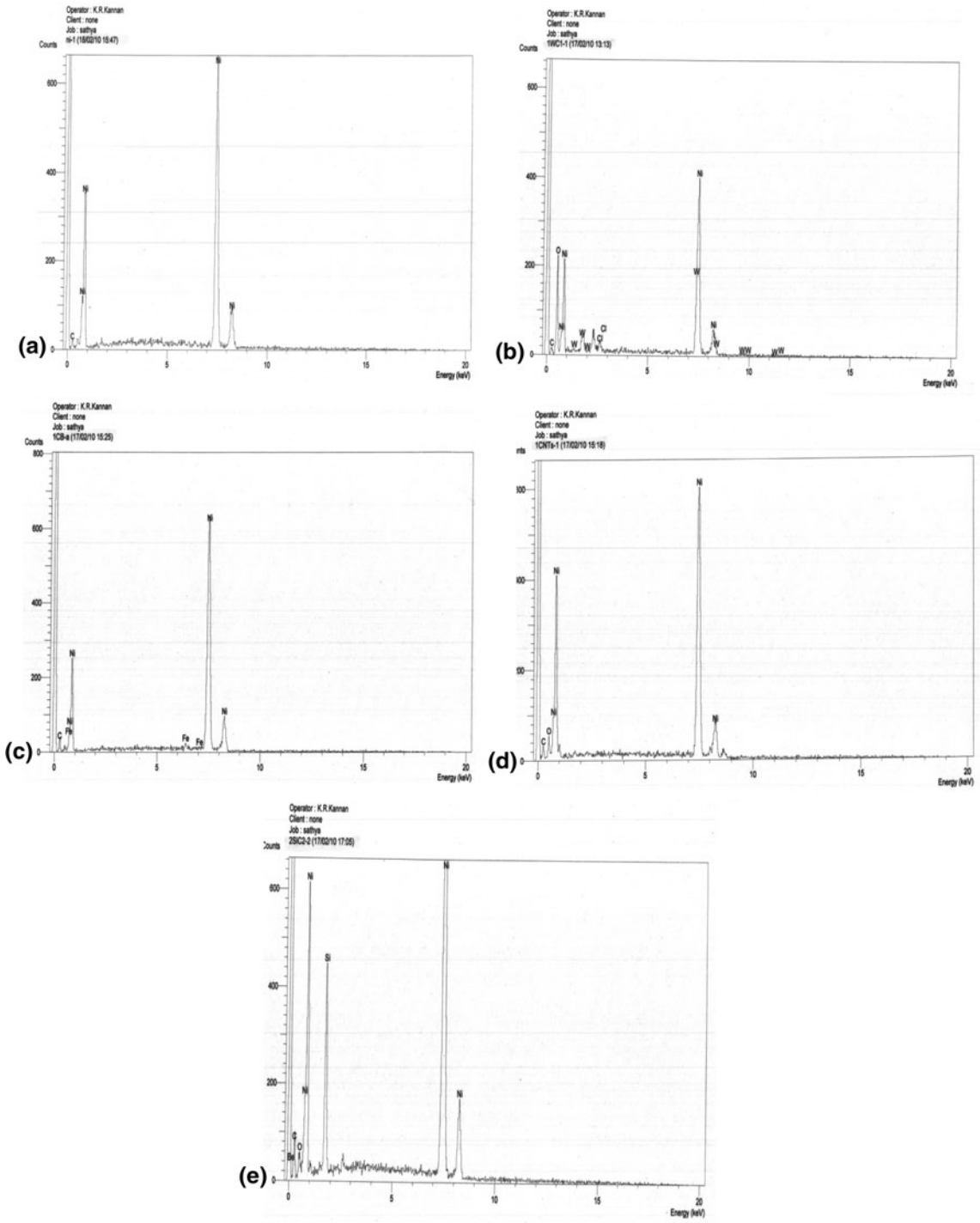


**Fig. 3** EDXA signature of Ni-based coatings on MS plate. (a) Ni coating, (b) Ni-WC coating, (c) Ni-CB coating, (d) Ni-CNT coating, and (e) Ni-SiC coating

deposit in terms of reduction of residual stress and porosity (Ref 13).

Figure 4 shows the effect of reinforcement loading on the coating thickness of Ni-based composite deposits. The thicknesses of the coatings range from 24 to 65 μm, depending on the reinforcement type and load used. It was observed that varying the reinforcement loading in the bath clearly affects the thickness of the coatings, and also varies with reinforcement. In all cases the coating thickness increased with increasing reinforcement loading. Ni-CNT showed the highest coating thickness due to the dimension and conductivity of CNT. Ni-SiC showed only marginal increment in coating thickness. The thickness of Ni-WC and Ni-CB was in between Ni-CNT and Ni-SiC composite coatings.

The WC, CB, CNT, and SiC have a hardening effect on the composite coating and hardness of the coating increases

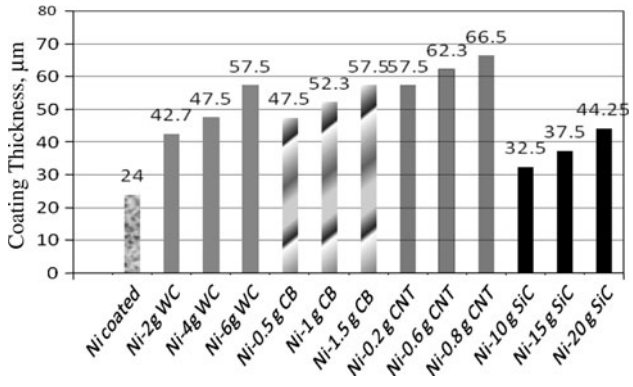


**Fig. 4** Coating thickness of uncoated, Ni-coated, and Ni-based composite coating on MS plate (loading g/L)

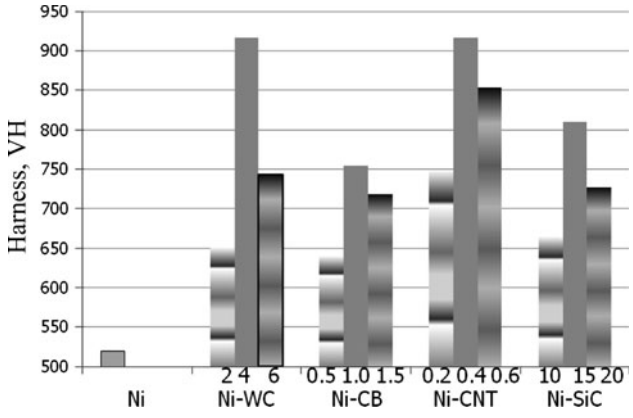


**Fig. 5** Microhardness of Ni-coated and Ni-based composite coating on MS plate (loading g/L)

from 510 kgf mm$^{-2}$ for pure Ni coating to 920 kgf mm$^{-2}$ (4 g/L WC and 0.4 g/L CNT) as observed in Fig. 5. The effect of reinforcement types and reinforcement content in the bath on the microhardness of the composites layers. The microhardness increased to a maximum and then decreased with reinforcement content. The grain-refining and dispersive strengthening effect become stronger with increasing reinforcement content, resulting in the microhardness of the Ni-based composite coatings increasing with larger reinforcement content. Ni-WC and Ni-CNT composite coatings showed higher hardness compared to other types. These results show improved both toughness and strength of the composites with co-deposition of WC/CNT's with nickel. Ni-CB composite coating showed lower hardness than the other three types of coatings. Ni-CB has more irregular surface finish as also more porosity that can be seen in the microstructure illustrated in Fig. 2(c). Ni-SiC composite coating hardness lies between Ni-CNT and Ni-CB due to its lower strength and lower SiC content in the coatings. The hardness increase noted in these composite coatings could be linked to a dispersion strengthening effect (Ref 14). With increasing the WC (4 g/L), CB (1.0 g/L), CNT (0.4 g/L), and SiC (15 g/L) content Ni composites coatings, the hardness was improved from 510 to 920, 760, 920, and 810 vH. However, the hardness dropped

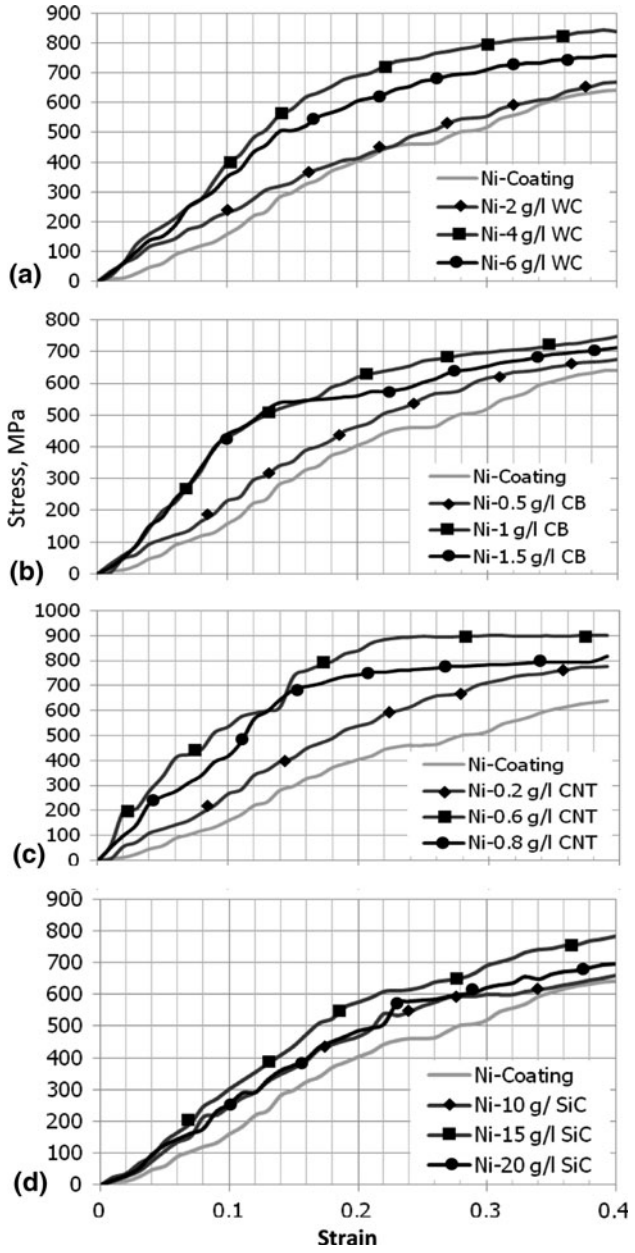


**Fig. 6** Tensile stress-strain diagram for Ni based composite coatings. (a) Ni-WC, (b) Ni-CB, (c) Ni-CNTs, and (d) Ni-SiC composite coatings

drastically to 750, 720, 850, and 730 vH for the specimen with the 6 g/L WC, 1.5 g/L CB, 0.6 g/L CNT, and 20 g/L SiC, respectively. This might be due to the porous microstructure of the higher loading composites.

The stress strain curves of the Ni-WC coatings (Fig. 6a), Ni-CB coatings (Fig. 6b), Ni-CNT (Fig. 6c), and Ni-SiC (Fig. 6d) are compared with pure Ni coating. For all tests the strain was determined by a sudden drop in the flow curve (catastrophic failure of coatings). Figure 6 shows the addition of reinforcement significant contribution on the composite coating behavior. In pure Ni coating curves show sooth behavior, which due to dynamic recovery and re-crystallization process occurring within the coating. For composite coatings,

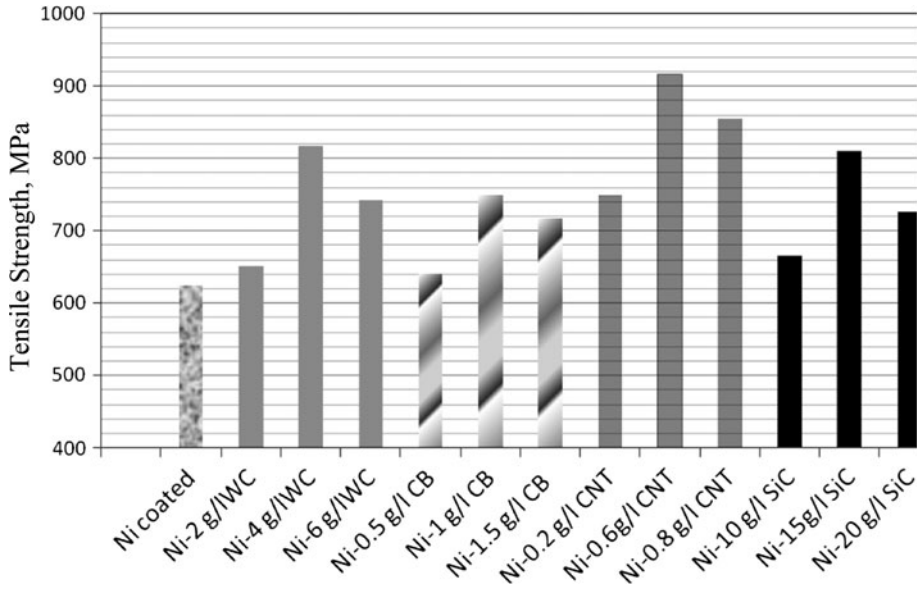


**Fig. 7** Tensile strength of uncoated, Ni-coated, and Ni-based composite coating on MS plate

the apparent softening after a strain of 0.2 is due to micro-crack formation at the specimen surface and in the interior as shown in Fig. 6. All graphs clearly show an increase in tensile strength, compared to pure Ni coating with the addition of reinforcement. The composite coating containing WC and CNT show the tensile strength was significantly higher than pure Ni coating, but SiC and CB coating show only a nominal increase in tensile strength. This can be attributed to the higher propensity of particle fracture in Ni-SiC composite coating.

Variation in bath loading and reinforcements were found to have a significant effect on the tensile properties of the composites. Figure 7 shows the variation of the tensile strength with different reinforcements and bath loading. It is also important to note that the reinforced particulate clusters also have a significant effect on the tensile properties of the composites coating. With increase in the WC (4 g/L), CB (1.0 g/L), CNT (0.4 g/L), and SiC (15 g/L) content in Ni composites coatings, the tensile strength improved from 620 to 810, 740, 910, and 808 MPa respectively. However, the tensile strength dropped to 740, 710, 860, and 710 MPa for the specimen with the 6 g/L WC, 1.5 g/L CB, 0.6 g/L CNT, and 20 g/L SiC, respectively. Increase in reinforcement (WC, CB, SiC, and CNT) loading into the bath caused more particles clustering as seen in coated materials.

XRD diagrams of the Ni and Ni-based coatings are shown in Fig. 8. The average crystal size of the coating was 43, 10.3, 9.1, 8.2, and 13, 5 nm for Ni, Ni-WC, Ni-CB, Ni-CNT, and Ni-SiC composite coatings, respectively. Fine-grained deposits are generally obtained at higher rate of formation of nuclei (Ref 15). The addition of reinforcement may provide a larger number of cathodic sites and consequently more number of fresh nuclei are formed on the metal surface. This results in a fine-grained composite deposit.

It is apparent that the diffraction pattern of pure Ni deposit is characterized by the intense (200) diffraction line corresponding to a (100) texture shown in Fig. 8(a), where the diffraction pattern of Ni-WC (Fig. 8b), Ni-CB(Fig. 8c), Ni-CNT (Fig. 8d), and Ni-SiC(Fig. 8e) reinforcements is characterized by (311) and (111) lines accompanied with an attenuation of the (200) line (Ref 7). It is of interest to note that the reinforcement of lines (311) and (111) are attributed to a dispersed (211) orientation (Ref 7). Hence, the composite coatings show maximum strength and hardness. The other reason for improvement in the strength is the reduction of grain size of Ni crystallites due to the presence of reinforcement in the composite coatings as compared with those of pure Ni coatings.

## 4. Fracture Surface

Figure 9 shows the morphology of the cracked samples after fracture (left and right figures represents lower and higher magnifications). The fracture surface of Ni coating (Fig. 9a) specimen shows an even crack approximately 10 μm in size indicative of an irregular shaped ductility failure. Figure 9(b) shows Ni-WC coated fracture surface, where cracks are deep and irregular with no plastic deformation. The cracks are initiated at Ni-WC interface and propagate through the interface and link up with other cracks that cause failure of the coating. The cracks in Ni-CB coating commence from the interparticles porosity in coating while pulling off test machine is loaded to a certain extent and propagate through the particle boundaries. Fractures occur in vulnerable regions of the coating as shown in Fig. 9(c), where the cleavage fractures with river patterns are dominant without dimples at the ductile matrix. One can see that the CNT produce modifications in the fracture surface aspect of the marks developed at the matrix surface as shown in Fig. 9(d). The cracks occur perpendicular

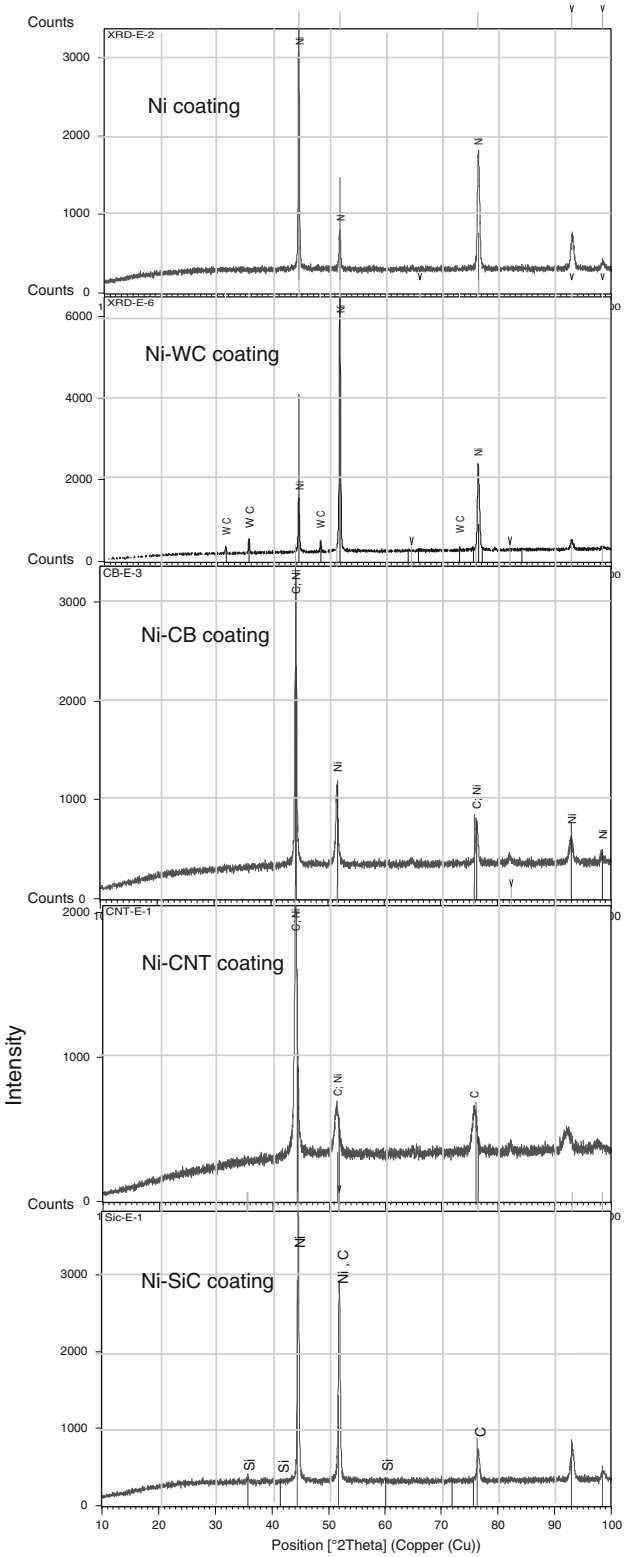


**Fig. 8** XRD patterns of (a) Ni, (b) Ni-WC, (c) Ni-CB, (d) Ni-CNT, and (e) Ni-SiC composite coatings on MS plates

to projectile direction but the perpendicular cracks are narrow and smaller. Figure 9(e) shows wide cracks on the surface which are perpendicular to the loading axis due the sharp edges of the SiC particles which indicate that the adhesion between the particles and matrix.

## 5. Conclusion

- This study shows that the WC, CB, CNT, and SiC can be co-deposited with nickel to improve the microhardness and tensile strength of the substrate.

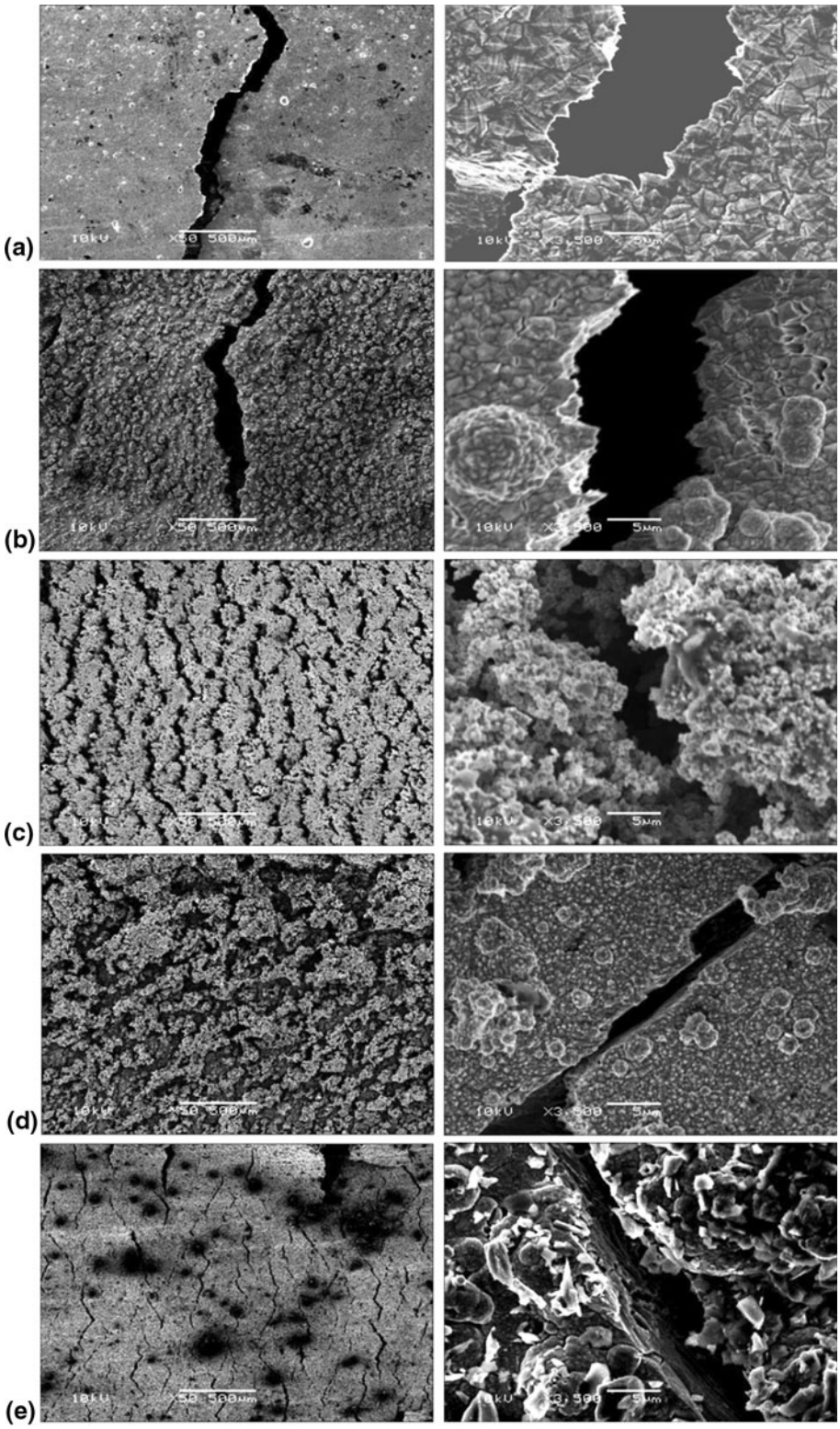


**Fig. 9** Fracture surface of Ni-based coatings on MS plate. (a) Ni coating, (b) Ni-WC coating, (c) Ni-CB coating, (d) Ni-CNT coating, and (e) Ni-SiC coating (500 and 5 μm)

- The increased hardness and tensile strength observed were due to solid loading and grain refinement of nickel.
- CNT and WC showed better reinforcing action than other two reinforcements.
- Ni-0.4 g/L CNT and Ni-4 g/L WC composites coatings exhibit improved mechanical properties compared with pure Ni and other Ni composites coatings.

## References


1. E. Eliaz, T.M. Sridhar, and E. Gileadi, Synthesis and Characterization of Nickel Tungsten Alloys by Electrodeposition, *Electrochim. Acta*, 2005, **50**, p 2893–2904
2. W.S. Zhao, N.R. Tao, J.I. Guo, Q.H. Lu, and K. Lu, High Density Nano-Scale Twins in Cu Induced by Dynamic Plastic Deformation, *Scripta Mater.*, 2005, **53**, p 745–749
3. C. Guo, Yu Zuo, X. Zhao, J. Zhao, and J. Xiong, The Effect of Electrodeposition Current Density on Properties of Ni-CNTs Composite Coatings, *Surf. Coat. Technol.*, 2008, **202**, p 3246–3250
4. P.-Q. Dai, W.-C. Xu, and Q.-Ya. Huang, Mechanical Properties and Microstructure of Nanocrystalline Nickel-Carbonnanotube Composites Produced by Electrodeposition, *Mater. Sci. Eng. A*, 2008, **483–484**, p 172–174
5. Y.S. Jeon, J.Y. Byun, and T.S. Oh, Electrodeposition and Mechanical Properties of Ni-Carbon Nanotubes Nanocomposite Coatings, *J. Phys. Chem. Solid*, 2008, **69**, p 1391–1394
6. B.M. Praveen and T.V. Venkatesh, Generation and Corrosion Behavior of Zn-Nano Sized Carbon Black Composite Coating, *Int. J. Electrochem. Sci.*, 2009, **4**, p 258–266
7. E.A. Pavlatou, M. Stroumbouli, P. Gyftou, and N. Spyrellis, Hardening Effect Induced by Incorporation of SiC Particles in Nickel Electrodeposits, *J. Appl. Electrochem.*, 2006, **36**, p 385–394
8. H.B. Temam, L. Zeroual, A. Chala, S. Rahmane, and C. Nouveau, Microhardness and Corrosion behavior of Ni-SiC Electrodeposited Coatings, *Plasma Process Polym.*, 2007, **4**, p 5618–5621
9. M. Surender, B. Basu, and R. Balasubramaniam, Wear Characterization of Electrodeposited Ni-WC Composites Coatings, *Tribol. Int.*, 2004, **37**, p 743–749
10. Y.S. Jeon, J.Y. Byun, and T.S. Oh, Electro Deposition and Mechanical Properties of Ni-Carbon Nanotube Nanocomposites Coatings, *J. Phys. Chem. Solids*, 2008, **69**, p 1391–1394
11. L. Shi, C. Sun, P. Gao, F. Zhou, and W. Liu, Mechanical Properties and Wear and Corrosion Resistance of Electrodeposited Ni-Co/SiC Nanocomposite Coating, *Appl. Surf. Sci.*, 2006, **252**, p 3591–3599
12. V. Medeliene and A. Kosenko, Structural and Functional properties of Electrodeposited copper Metal matrix Composite coating with Inclusions of WC, *Mater. Sci.*, 2008, **14**(1), p 29–33
13. H. Hhiriac, A.E. Moga, C. Gherasim, and N. Lupu, Synthesis and Characterization of Fe-W and Ni-W Composite Coatings, *Rom. J. Inf. Sci. Technol.echnology*, 2008, **11**(2), p 123–132
14. Y. Boonyongmaneerat, K. Saengkiettiyut, S. Saenapitak, and S. Sangsuk, Effect of WC Addition on Structure and Hardness of Electrodeposited Ni-W, *Surf. Coat. Technol.*, 2009, **203**, p 3590–3594
15. C.S. Lin and K.C. Huang, Codeposition and Microstructure of Nickel-SiC Composite Electrodeposited from Sulphamate Bath, *J. Appl. Electrochem.*, 2004, **34**, p 1013–1029